

# DWT-SATS Based Detection of Image Region Cloning

Michael Zimba

**Abstract**—A duplicated image region may be subjected to a number of attacks such as noise addition, compression, reflection, rotation, and scaling with the intention of either merely mating it to its targeted neighborhood or preventing its detection. In this paper, we present an effective and robust method of detecting duplicated regions inclusive of those affected by the various attacks. In order to reduce the dimension of the image, the proposed algorithm firstly performs discrete wavelet transform, DWT, of a suspicious image. However, unlike most existing copy move image forgery (CMIF) detection algorithms operating in the DWT domain which extract only the low frequency subband of the DWT of the suspicious image thereby leaving valuable information in the other three subbands, the proposed algorithm simultaneously extracts features from all the four subbands. The extracted features are not only more accurate representation of image regions but also robust to additive noise, JPEG compression, and affine transformation. Furthermore, principal component analysis-eigenvalue decomposition, PCA-EVD, is applied to reduce the dimension of the features. The extracted features are then sorted using the more computationally efficient Radix Sort algorithm. Finally, same affine transformation selection, SATS, a duplication verification method, is applied to detect duplicated regions. The proposed algorithm is not only fast but also more robust to attacks compared to the related CMIF detection algorithms. The experimental results show high detection rates.

**Keywords**—Affine Transformation, Discrete Wavelet Transform, Radix Sort, SATS.

## I. INTRODUCTION

A copy-move image forgery, CMIF, is a specific kind of image tampering. In a CMIF, a part of an image is copied and then pasted on a different location within the same image. Usually, such an image tampering is done with the aim of either hiding some image details, in which case a background is duplicated, or adding more details in which case at least an object is cloned. Fig. 1 depicts examples of CMIF attacks.

The forged images are shown in the left column and the original images are shown in the right column. The top row depicts object removal and the bottom row shows object duplication in an image attacked by CMIF.

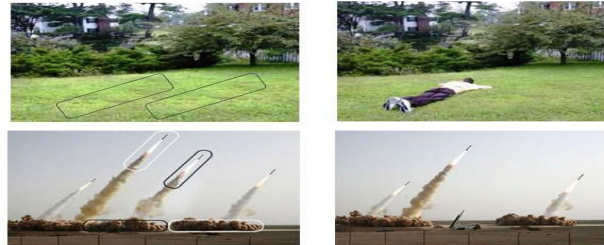


Fig. 1 Examples of CMIF. Forged images are in left column and original images are in right column. Rows depict object removal (above) and object duplication (below)

CMIF attacks are often imperceptible because of the fact that the copied regions come from the same image as the segments where the regions are pasted thereby making the color palettes, noise components, dynamic ranges and other properties compatible with the rest of the image [1], [2]. Furthermore, an attacker can geometrically manipulate, compress or add noise to the copied regions thereby mating and blending the pasted regions into their targeted surroundings [3], [4].

The primary task of a CMIF detection algorithm is to determine if a given image contains cloned regions without prior knowledge of their shape and location. Various passive forensic methods have been designed to detect CMIF [2]-[6]. However, we narrow down our presentation to only those CMIF detection algorithms which utilize block characteristic approach in their extraction of the feature vectors.

Luo et al. [7] propose a CMIF detection method in which a suspicious  $M \times N$  image is tiled with overlapping  $b \times b$  blocks. In total,  $k = (M - b + 1)(N - b + 1)$  blocks are needed in order to cover the whole image. A 7-tuple feature vector is defined to represent each of the  $k$  blocks. The first three components of each feature vector consist of the averages of the pixel intensities in the whole block. The block is then divided into halves horizontally, vertically, main-diagonally and minor-diagonally. The last four components of the feature vector are the ratios of the sums of pixel intensities in one half of the block, in each demarcation direction, to the sum of pixel intensities in the whole block. Because the components of the feature vectors are floating numbers, Lexicographic Sort is used in ordering the feature vectors. Then shift vector method is used to verify region duplications. The first weakness of the algorithm proposed by Luo et al. [7] is the fact that it is applied to images in spatial domain where the dimensions of images cannot be reduced without significant loss of information. Secondly, the slower Lexicographic Sort used in

M. Zimba is with the Department of Physics, Mzuzu University, Private Bag 201, Luwingu, Mzuzu 2, Malawi (Phone: +265 1320 575; fax: +265 1320 568; e-mail: mgmzimba@gmail.com).

ordering the feature vectors raises the complexity of the algorithm to  $O(7k \log k)$ . At the same time the extracted feature vectors are not robust to geometric attacks. In addition, the algorithm inherits the fundamental weakness of the shift vector approach of failing to detect geometrically manipulated regions. It follows that the method is not only complex but also weak to attacks.

Following a similar approach, Lin et al. [8] define a 9-tuple feature vector whose components also consist of block based statistics of the pixel intensities. Through floor operation, the components are rounded into integers. Consequently Radix Sort is used to sort the feature vectors and it improves the computational complexity of the algorithm to  $O(9k)$ . However, the algorithm has the same weaknesses as those of the algorithm proposed by Luo et al. [7], minus Lexicographic Sort.

In Section II, a focused and comprehensive background towards the design of the proposed algorithm is presented. The proposed CMIF detection algorithm is presented in Section III. Its advantages over existing related CMIF algorithms are stipulated. Section IV presents the detection results by the proposed algorithm and Section V concludes the paper.

## II. BACKGROUND

### A. Principal Component Analysis

Principal Component Analysis, PCA, is a well known technique for multivariate analysis [5], [9]. The core task of PCA is to reduce the dimensionality of a data set which has a large number of interrelated variables, while retaining the original variations of the data as much as possible. For a positive semi-definite symmetric matrix, finding principal components is computationally the same as solving an eigenvalue-eigenvector problem. From this perspective, we now present principal component analysis-eigenvalue decomposition, PCA-EVD, as an algebraic tool for matrix dimension reduction. Let  $H$  denote a matrix defined in (1) as follows:

$$H = \begin{bmatrix} \rightarrow \\ a_1 \\ \rightarrow \\ a_2 \\ \vdots \\ \rightarrow \\ a_n \end{bmatrix} = \begin{bmatrix} a_{11} & a_{12} & \cdots & a_{1b} \\ a_{21} & a_{22} & \cdots & a_{2b} \\ \vdots & \vdots & \ddots & \vdots \\ a_{n1} & a_{n2} & \cdots & a_{nb} \end{bmatrix} \quad (1)$$

If we guarantee that each of the row vectors of the matrix  $H$  is zero mean, and we let  $\mu_j, \lambda_j$  be a pair of corresponding eigenvector and eigenvalue respectively such that  $j=1,2,\dots,b$  and  $\lambda_1 \geq \lambda_2 \geq \dots \geq \lambda_b$ , then (2) and (3) are clear, where  $C$  is a covariance matrix of the matrix  $H$ .

$$C = \sum_{i=1}^n \vec{a}_i \vec{a}_i^T \quad (2)$$

$$C \vec{\mu}_j = \lambda_j \vec{\mu}_j \quad (3)$$

Considering a new linear basis formed by the eigenvectors,  $\mu_j$ , (4) shows that we can reduce the dimension of the row vectors of  $H$  to  $t \leq b$  without much loss of original information.

$$\vec{a}_i = \sum_{j=1}^{t \leq b} \vec{a}_i^T \vec{\mu}_j \vec{\mu}_j \quad (4)$$

### B. Same Affine Transformation Selection

The idea of recovering parameters of affine transformation of a region in an image was once presented by Amerini et al. [10]. In their work [10], the authors use Maximum Likelihood estimation of homography [11] to estimate the parameters of the affine transformation in homogenous coordinates.

However, a simple and straight forward approach to recovering the parameters of the affine transformation of a region in an image in 2D Cartesian coordinates, named the same affine transformation selection, SATS, is proposed by Christlein et al. [12]. SATS is an alternative selection and verification method to the common shift vector method [1]. Like shift vector, SATS has an outlier filtering property. However, SATS is insensitive to affine transformation in that it recovers the affine transformation parameters of a geometrically manipulated region at a cost of only a slightly increased computational time. Hence SATS is a better option for the verification of the duplicated regions which have been affected by translation, rotation or scaling. The detailed SATS method is as follows:

Let  $B_{i1}$  and  $B_{i2}$  be  $b \times b$  matching blocks whose centers, in row vector form, are  $\vec{c}_{i1}$  and  $\vec{c}_{i2}$  respectively. If  $B_{i2}$  is a result of an affine transformation of  $B_{i1}$  then

$$\vec{c}_{i2} = \vec{c}_{i1} \cdot A + \vec{s}, \quad (5)$$

The  $2 \times 2$  matrix  $A$  in (5) consists of the two rotation and two scaling parameters and the vector  $\vec{s}$  consists of the two translation parameters. Let  $\vec{h}_i = (\vec{h}_{i1}, \vec{h}_{i2})$  be a vector of the feature vectors  $\vec{h}_{i1}, \vec{h}_{i2}$  extracted from the matching blocks  $B_{i1}$  and  $B_{i2}$  respectively, then a set of three such vectors as

$\vec{h}_i$  is enough to initially approximate all the six parameters of the affine transformation. More such vectors may be needed only to stabilize the parameter approximation. This is the core purpose of the SATS algorithm. For a detailed presentation of the SATS algorithm refer to [12], [13].

### C. Block Characteristic Based Feature Extraction

A given feature vector  $\vec{h} = h_1 h_2 \dots h_t$ , whose components  $h_i, i=1,2,\dots,t$  are individual pixels or normalized DWT coefficients, is sensitive to pixel variations induced by additive

noise and lossy compression, [14]. The probable solution to this drawback is to use feature vectors whose components are block characteristics of the pixels, instead of the individual pixels. Clustering the pixels into blocks has some quantizing effect on the components thereby making the feature vectors more robust to pixel changes induced by additive noise and lossy compressions. We now establish the quantizing effect and robustness of the block characteristic approach. Fig. 2 shows a  $b \times b$  block divided into four concentric squares.

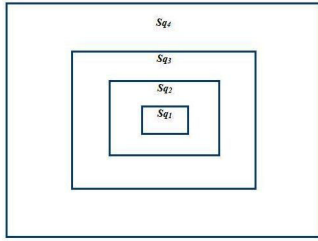


Fig. 2 Block division into four concentric squares

Suppose we define a feature vector,  $\vec{h} = h_1 h_2 \dots h_5$ , in which the individual components  $h_i, i=1,2,\dots,5$  are computed as follows:

- (i) Let  $a_1$  be the average of the pixel intensities within the whole block, then  $h_1 = a_1$
- (ii) The block is then divided into 4 concentric squares  $sq_i, 1 \leq i \leq 4$  of sides  $\left\lfloor \frac{b}{4} \right\rfloor \times i + 1, 1 \leq i \leq 4$  respectively.  $\lfloor \cdot \rfloor$  is the floor operator.
- (iii) Let  $ave(sq_i)$  be the average of pixel intensities within the square,  $sq_i$ , then  $h_{i+1} = ave(sq_i), 1 \leq i \leq 4$ .

The defined components will not significantly change with pixel variations induced by additive noise and lossy compression. For example, assuming that the per pixel additive white Gaussian noise (AWGN) for each pixel,  $\delta$ , is an independent and identically distributed variable from a zero-mean normal distribution with variance  $n$ . Then the noisy block due to addition of such noise will be  $B' = B + \delta$ . Consequently, the average of the noisy block will be  $a'_1 = a_1 + \delta^1$  where  $E(\delta^1) = 0$  and  $D(\delta^1) = \frac{n}{b^2}$ . If  $b \geq 5$ , then  $a'_1 \approx a_1$ . This means that  $h_1$  does not change much. Hence  $h_1$  is robust to such noise addition. Extending the argument for the robustness of  $h_1$  to  $h_i, 2 \leq i \leq 5$  is obvious.

Hence  $\vec{h} = h_1 h_2 \dots h_5$  is robust to additive noise. At the same time, JPEG compression and Gaussian blurring only slightly change the low frequency components of the image signal and discard high frequency components. Hence  $\vec{h} = h_1 h_2 \dots h_5$  is also robust to these operations. Furthermore the feature vector  $\vec{h} = h_1 h_2 \dots h_5$  is robust to affine transformation. For example,

let the block  $B'$  be the result of rotating the block of Fig. 2 through  $90^\circ$  clockwise and let  $sq'_1, sq'_2, sq'_3$  and  $sq'_4$  be concentric squares of  $B'$ , then it is clear that  $sq'_i = sq_i, 1 \leq i \leq 4$ . It follows that the feature vector  $\vec{h} = h_1 h_2 \dots h_5$  is robust to such a rotation. The argument also holds, practically, for rotation through arbitrary angles because the majority of each square's populace will still be within the square at any rotation.

#### D. The Radix Sort

Let  $\vec{V} = v_1 v_2 \dots v_d$  and  $\vec{U} = u_1 u_2 \dots u_d$  be  $d$ -tuple sequences such that  $v_i$  and  $u_i$  are the  $i$ -th dimensions of  $\vec{V}$  and  $\vec{U}$  respectively. Let  $K_i$  compare  $\vec{V}$  and  $\vec{U}$  by their  $i$ -th dimension. Let  $StableSort(H, K)$  be any stable sorting algorithm such as Bucket-Sort that uses the comparator  $K$ . If we let  $K = N$  be integer keys in the range  $[0 - (N-1)]$ , then the sorting method which uses the sorting algorithm  $StableSort(H, N)$  to lexicographically order  $\vec{V} \leq \vec{U}$  for every pair  $\vec{V}$  and  $\vec{U}$  in  $H$ , where  $H$  is a set of  $k$   $d$ -tuple sequences, is the Radix Sort. The application of the Radix Sort obviously requires that  $v_i$  and  $u_i$  be integers in the range  $[0 - (N-1)]$  for every comparison of  $d$ -tuple sequences  $\vec{V} = v_1 v_2 \dots v_d$  and  $\vec{U} = u_1 u_2 \dots u_d$  in the set  $H$ . The concise presentation of the Radix Sort is shown in Table I.

TABLE I  
THE RADIX SORT

|   |
|---|
| <b>Input:</b> $d$ -tuple sequences in $H$ such that $(0, \dots, 0) \leq (v_1, \dots, v_d)$ and $(v_1, \dots, v_d) \leq (N-1, \dots, N-1)$ for each tuple $\vec{V}$ in $H$ . |
| <b>Output:</b> Set $H$ sorted in Lexicographic order.   |
| <b>For</b> $i \leftarrow d$ <b>down to</b> 1  |
| $Stable-sort(H, N)$   |

In this presentation,  $d$  is the length of the keys. Let  $O(T(k))$  be the complexity of the  $StableSort(H, N)$ , if we let  $StableSort(H, N)$  be the  $BucketSort(H, N)$ , then  $O(T(k)) = O(N + k)$ . It follows that the Radix Sort has the complexity  $O(d(N + k))$ . If  $k \gg N$ , then  $O(d(N + k)) \approx O(dk)$ .

### III. THE PROPOSED ALGORITHM

The proposed CMIF detection algorithm operates in the DWT domain of a suspicious image and it consists of the following steps. It is important to emphasize, right at the beginning, that the proposed algorithm is not restricted to images in the red, green, blue, RGB color model. Any color model can apply. Besides, multi-channel images can readily be transformed between color spaces. For mono-chromatic

images, there is no harm in repeating some components of the extracted feature vectors.

1. Let  $F(x, y)$  be a suspicious RGB image with  $k_3 = M \times N$  pixels per channel.
2. Initialize the following parameters:
  - (i)  $b \times b$ , the block size.
  - (ii)  $t$ , the PCA truncation threshold.
  - (iii)  $l$ , the level of orientation.
  - (iv)  $t_1$ , separation threshold.
  - (v)  $t_2$ , connectivity threshold.
3. Perform an  $l$ -level DWT on the  $F(x, y)$  to obtain subbands  $F_\alpha^l(u, v)$  where  $\alpha \in \{LL, LH, HL, HH\}$  represents orientation and a positive integer  $l$  is the level of the orientation. Each  $F_\alpha^l(u, v)$  has a reduced image space of  $k_2 = r \times c \approx \frac{k_3}{4^l}$  pixels. The pixels are actually DWT coefficients normalised to unsigned integers in the range  $[0-255]$ .
4. Slide a fixed  $b \times b$  window on every  $F_\alpha^l(u, v)$  pixel by pixel from top-left corner to bottom-right corner, in a raster scan order, resulting in a total of  $4 \times k_1 = 4 \times (r - b + 1)(c - b + 1)$  overlapping blocks. For each of the  $k_1$  block locations, compute the feature vectors  $\vec{h}^\alpha = h_1^\alpha h_2^\alpha \dots h_7^\alpha$ ,  $\alpha \in \{LL, LH, HL, HH\}$  and  $\vec{h} = h_1 h_2 \dots h_{28}$  as follows
  - (i) Let  $a_i^\alpha$ ,  $1 \leq i \leq 3$ , be the averages of red, green and blue channels of  $F_\alpha^l(u, v)$ ,  $\alpha \in \{LL, LH, HL, HH\}$  respectively, then  $h_i^\alpha = a_i^\alpha$ ,  $1 \leq i \leq 3$ .
  - (ii) Compute the  $Y$  channel of  $F_\alpha^l(u, v)$ ,  $\alpha \in \{LL, LH, HL, HH\}$  using the relationship  $Y = 0.299R + 0.587G + 0.114B$ .
  - (iii) Divide each block in the  $Y$  channel into 4 concentric squares  $sq_i^\alpha$ ,  $1 \leq i \leq 4$  of sides  $\left\lfloor \frac{b}{4} \right\rfloor \times i + 1$ ,  $1 \leq i \leq 4$  according to Section II.
  - (iv) Consider only pixels inside each concentric squares  $sq_i^\alpha$ ,  $1 \leq i \leq 4$  sequentially. Then  $h_{i+3}^\alpha = ave(sq_i^\alpha)$ ,  $1 \leq i \leq 4$  where  $ave(sq_i^\alpha)$  is the average of the pixels inside the square,  $sq_i^\alpha$ .
  - (v) Compute  $\vec{h} = h_1 h_2 \dots h_{28} = \vec{h}^{LL} \vec{h}^{LH} \vec{h}^{HL} \vec{h}^{HH}$  by concatenating the four vectors  $\vec{h}^\alpha = h_1^\alpha h_2^\alpha \dots h_7^\alpha$ ,  $\alpha \in \{LL, LH, HL, HH\}$ .
  - (vi) Form a  $k_1 \times 28$  matrix  $H$  whose rows are the  $k_1$  feature vectors,  $\vec{h} = h_1 h_2 \dots h_{28} = \vec{h}^{LL} \vec{h}^{LH} \vec{h}^{HL} \vec{h}^{HH}$ .
5. Perform PCA-EVD on the matrix  $H$  to reduce the dimension of the features vectors to  $t < 28$  according to

Section II.

6. Normalize each of the  $t$  components of each row of the matrix  $H$  to unsigned integers in the range  $[0 - 255]$ .
7. Sort the rows of the matrix  $H$  using Radix Sort.
8. Performed SATS algorithm on the sorted matrix  $H$  to verify region duplications and to filter out outliers.
9. Finally, filter out isolated matching blocks through morphological opening to obtain the final results.

The following are the advantages of the proposed algorithm over existing CMIF detection algorithms. 1) Normally, the computational complexity of a CMIF detection algorithm converges to the complexity of the feature sorting method which in turn is a function of the dimensions of the image. Consequently, most CMIF detection methods which operate in the spatial domain are generally more complex [1], [15]. In order to reduce the dimension of the image, most existing CMIF detection algorithms which operate in the DWT domain [1], [2], [16] approximate the image by extracting only the low frequency subband  $F_{LL}^l(u, v)$ . Much as most of the energy of an image is concentrated in the subband  $F_{LL}^l(u, v)$ , valuable detail information of the image is still lost by ignoring the other three subbands. In the proposed algorithm, we manage to incorporate information from all the four subbands thereby making the extracted features more accurate representation of the blocks. In this case, two blocks can only have matching features if and only if they are similar in all the subbands of the DWT of an image. Meanwhile, the number of blocks,  $k_1$ , just before the feature sorting algorithm is applied is the same as in any other CMIF detection algorithm operating in the DWT domain. Therefore we incur the same sorting costs as the existing CMIF algorithms in the DWT domain. 2) In addition, the proposed algorithm also reduces the dimension of each feature vector from  $1 \times 28$  to  $1 \times t$  through PCA-EVD. This overly reduces the complexity of the algorithm. 3) Remarkable reduction in complexity of the proposed algorithm is achieved through sorting extracted features using the Radix Sort which has the complexity of  $O(tk_1)$  instead of the common Lexicographic Sort which would have the complexity of  $O(7k_1 \log k_1)$  for the same task. 4) At the same time, the extracted features are robust to additive noise, JPEG compression, Gaussian blurring and affine transformation. 5) Finally, a SATS approach is taken at the duplication verification stage thereby avoiding the fundamental weakness of the common shift vector approach of failing to detect geometrically manipulated duplicated regions. SATS is insensitive to affine transformation. Therefore, the proposed algorithm is not only non-complex but also robust to linear and geometric attacks.

#### IV. EXPERIMENTAL RESULTS

To validate the proposed algorithm, experiments are conducted on a dataset of 300 images sourced mostly from [www.freefoto.com](http://www.freefoto.com). Most images have the dimensions of  $256 \times 256$  pixels. When a 1-level DWT, Haar, is performed on the images, the dimensions of the images reduce to

$128 \times 128$  pixels. The level of orientation is restricted to  $l = 1$ . The size of the block is set to  $b \times b = 17 \times 17$  pixels throughout the experiments. The PCA-EVD truncation threshold is set to  $t = 8$ . The distance of the matching block pairs is set to  $t_1 = 17$  and the least frequency of connected matches is set to  $t_2 = 50$ .

Fig. 3 shows examples of the detection results by the proposed algorithm. In the right column are the original images; in the middle column are the forged images in which the duplicated regions are affected by various attacks; the right column shows the results from the proposed algorithm.

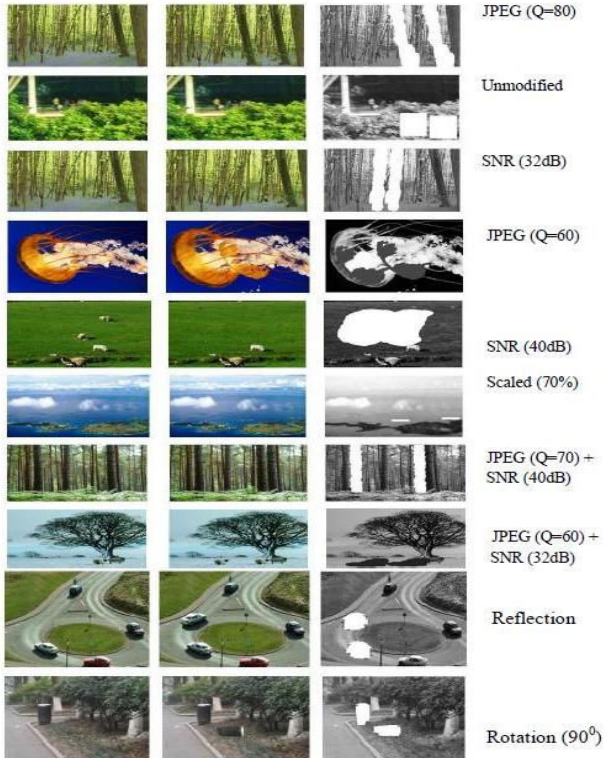


Fig. 3 Detection results by the proposed algorithm

We assess the performance of the proposed CMIF algorithm using the following stricter method. Let  $D_1$  and  $D_2$  be an original region and a duplicated region respectively,  $R_1$  and  $R_2$  be the respective output regions mapped by the proposed algorithm, then the accuracy  $r$  and false negative  $w$  of the detection are respectively defined in (6) and (7) as follows:

$$r = \frac{|R_1 \cap D_1| + |R_2 \cap D_2|}{|D_1| + |D_2|} \quad (6)$$

$$w = \frac{|R_1 \cup D_1| + |R_2 \cup D_2|}{|D_1| + |D_2|} - r \quad (7)$$

The results by the proposed algorithm for the set of 300 images whose duplicated regions are affected by various forms of attacks are shown in Table II. The results demonstrate that the algorithm has, on average, recommendable accuracy in cases where the duplicated regions are merely translated or reflected. High detection rates are also registered in cases where the duplicated regions are affected by JPEG compression or additive noise. There is a fairer accuracy where the duplicated regions are affected by rotation, or combined forms of affine transformation. The accuracy of the algorithm is relatively low in cases where duplicated regions are affected by scaling or rotation through arbitrary angles. In general, however, we note that the accuracy of the algorithm increases with an increase in the size of the duplicated regions.

TABLE II  
RESULTS OF THE PROPOSED ALGORITHM FOR A SET OF 300 IMAGES

| Forms of Attacks            | Average Detection Rates of Duplicated Regions of Various Sizes (pixels) and Forms of Attacks |        |         |        |         |        |
|-----------------------------|--|--------|---------|--------|---------|--------|
|                             | 32 × 32  |        | 48 × 48 |        | 64 × 64 |        |
|                             | $r$  | $w$    | $r$     | $w$    | $r$     | $w$    |
| Translation                 | 1.0000   | 0.0567 | 1.0000  | 0.0521 | 1.0000  | 0.0311 |
| JPEG 100                    | 1.0000   | 0.0499 | 1.0000  | 0.0401 | 1.0000  | 0.0323 |
| Quality 80                  | 0.9987   | 0.0977 | 0.9993  | 0.0861 | 1.0000  | 0.0719 |
| 60                          | 0.9843   | 0.1301 | 0.9897  | 0.1245 | 0.9926  | 0.1171 |
| 40                          | 0.9695   | 0.1171 | 0.9702  | 0.1069 | 0.9818  | 0.1011 |
| SNR 40                      | 0.9976   | 0.1191 | 0.9983  | 0.1081 | 0.9995  | 0.0992 |
| (dB) 32                     | 0.9881   | 0.1293 | 0.9890  | 0.1137 | 0.9893  | 0.1017 |
| 24                          | 0.9537   | 0.1477 | 0.9594  | 0.1319 | 0.9663  | 0.1231 |
| 20                          | 0.8913   | 0.1484 | 0.8999  | 0.1407 | 0.9124  | 0.1295 |
| Scaled                      | 0.7447   | 0.4680 | 0.7653  | 0.4631 | 0.7818  | 0.4467 |
| Reflection                  | 0.9987   | 0.0734 | 0.9998  | 0.0614 | 1.0000  | 0.0231 |
| 60°                         | 0.8847   | 0.1461 | 0.9013  | 0.1213 | 0.9355  | 0.1193 |
| 90°                         | 0.9882   | 0.1314 | 0.9889  | 0.0978 | 0.9987  | 0.0953 |
| Rotation 120°               | 0.8959   | 0.1217 | 0.9153  | 0.1169 | 0.9454  | 0.1115 |
| Mixed affine transformation | 0.8863   | 0.1217 | 0.8991  | 0.1200 | 0.9114  | 0.1121 |

We take an extra effort to compare the proposed algorithm with the existing CMIF algorithms in terms of feature forms, feature vector sorting methods, number of blocks required to cover the whole image, and run time complexity. The comparison results are shown in Table III. For comparison purposes, consider a  $256 \times 256$  image tiled with  $8 \times 8$  overlapping blocks. Recall that  $k_1 \approx \frac{k}{4^l}$  where  $k = (M - b + 1)(N - b + 1)$ . Because the dimensions of the image are reduced through DWT and the dimensions of the feature vectors are reduced through PCA before the feature vectors are sorted using Radix Sort, the run time complexity of the proposed method is lower than those of the existing block-based methods.



TABLE III  
COMPARISON WITH EXISTING RELATED ALGORITHMS

| Algorithm      | Feature form                | Sorting Method     | Number of 8x8 Blocks $k$ | Run Time Complexity for Any Given $k$ |
|----------------|-----------------------------|--------------------|--------------------------|---------------------------------------|
| Luo et al. [7] | Pixel Block Characteristics | Lexicographic Sort | 62,001                   | $O(7 \log k)$                         |
| Lin et al. [8] | Pixel Block Characteristics | Radix Sort         | 62,001                   | $O(9k)$                               |
| Proposed       | DWT Block Characteristics   | Radix Sort         | 14,641                   | $O(8k_1)$                             |

## V. CONCLUSION

In this paper, an effective and robust CMIF detection method has been presented. The method is capable of detecting duplicated regions which are affected by additive noise, lossy compression and affine transformation attacks. In order to reduce the dimension of the image, the proposed algorithm performs DWT. However, unlike most existing algorithms operating in the DWT domain which extract only the low frequency subband of the DWT of a suspicious image thereby leaving valuable information in the other three subbands, the proposed algorithm simultaneously extracts features from all the four subbands. The extracted features are not only more accurate representation of image regions but also robust to additive noise, JPEG compression, and affine transformation. Furthermore, PCA-EVD is applied to reduce the dimension of the features. The extracted features are then sorted using the more efficient Radix Sort algorithm. Finally, SATS is applied to verify duplicated regions. SATS is opted for over the shift vector method because SATS is insensitive to affine transformation. Consequently, the proposed algorithm is not only fast but also more robust compared to the existing related algorithms. The experimental results show high detection rates.

## REFERENCES

- [1] H. Farid, "A Survey of Image Forgery Detection," in *Signal Proc. Magazine*, vol. 26, no. 2, 2009, pp.16-25.
- [2] A.C. Popescu and H. Farid, "Exposing Digital Forgeries by Detecting Traces of Resampling," *IEEE Trans. Signal Processing*, vol. 53, pp. 758-767, 2005.
- [3] H. Sencar and N. Memon, "Overview of State- of- the- art in Digital Image Forensics," *Algorithms, Architectures and Information Systems Security*, pp. 325-344, 2008.
- [4] T. Ng, S. Chang, C. Lin, and Q. Sun, "Passive-Blind Image Forensics," *Multimedia Security Technologies for Digital Rights Management*, Academic Press, pp. 383-412, 2006.
- [5] M. Zimba and S. Xingming, "DWT-PCA (EVD) Based Copy-move Image Forgery," *JDCTA: International Journal of Digital Content Technology and its Applications*, Vol. 5, No. 1, 2011, pp.251-258.
- [6] N. Wandjie, S. Xingming and M. Kue, "Detection of Copy-move Forgery in Digital Images based on DCT," *IJCSI*, Vol. 10, No 1, 2013, pp. 295-302.
- [7] W. Luo, J. Huang, and G. Qui, "Robust Detection of Region Duplication Forgery in Digital Image," *Proceedings of the 18<sup>th</sup> International Conference on Pattern Recognition*, Vol. 4, 2006, pp. 746-749.
- [8] H.J. Lin, C.W. Wang, and Y.T. Kao, "Fast Copy-Move Forgery Detection," *WSEAS Transactions on Signal Processing*, Vol. 5, No. 5, 2009, pp.188-197.
- [9] I.T. Jolliffe *Principal Component Analysis*, Springer-Verlag New York, 2<sup>nd</sup> edition, 2002, ch.1-4.
- [10] I. Amerini, L. Ballan, R. Caldelli, A.D. Bimbo and G. Serra, "Geometric Tampering Estimation by Means of a Sift-Based Forensic Analysis,"

*International Conf. Acoustic Speech and Signal Processing*, Dallas TX, USA, March 14-19, 2010.

- [11] R.I. Hartley and A. Zisserman, *Multiple View Geometry in Computer Vision*, Cambridge University Press, 2<sup>nd</sup> edition, 2004.
- [12] A.V. Christlein, C. Riess and E. Angelopoulou, "On Rotation Invariance in Copy-Move Forgery Detection," in *Proc. IEEE Workshop, Information Forensics and Security*, Seattle USA, 2010.
- [13] M. Zimba and D. Nyirenda, "Copy-Move Image Forgery Detection in Virtual Electrostatic Field" *ICECSP 2013: International Conference on Electronics, Control and Signal Processing*, Cape Town, South Africa, November (20-21), 2013, pp. 925-932.
- [14] M. Zimba and S. Xingming, "Fast and Robust Image Cloning Detection Using Block Characteristics of DWT Coefficients," *JDCTA: International Journal of Digital Content Technology and its Applications*, Vol. 5, No. 7, 2011, pp.359-367.
- [15] C. Riess and E. Angelopoulou, "Scene Illumination as an Indicator of Image Manipulation," *12<sup>th</sup> International Workshop on Information Hiding*, Springer, Vol. 6387, 2010, pp. 66-80.
- [16] G. Li, Q. Wu, D. Tu, and S. Sun, "A Sorted Neighborhood Approach for Detecting Duplicated Regions in Image Forgeries based on DWT and SVD," in *Proc. IEEE International Conf. Multimedia and Expo*, Beijing China, 2007, pp. 1750-1753.